Effective potentials of interactions and thermodynamic properties of a nonideal two-temperature dense plasma

T. S. Ramazanov, Zh. A. Moldabekov, and M. T. Gabdullin
Al-Farabi Kazakh National University, Institute of Experimental and Theoretical Physics, Almaty 050040, Kazakhstan
(Received 24 February 2015; revised manuscript received 16 June 2015; published 19 August 2015)

In this article a dense nonideal, nonisothermal plasma is considered. New effective screened interaction potentials taking into account quantum-mechanical diffraction and symmetry effects have been obtained. The effective potential of the ion-ion interaction in plasmas with a strongly coupled ion subsystem and semiclassical electron subsystem is presented. Based on the obtained effective potentials the analytical expressions for internal energy and the pressure of the considered plasma were obtained.

DOI: 10.1103/PhysRevE.92.023104 PACS number(s): 52.25.Kn

I. INTRODUCTION

Currently, many experimental and theoretical investigations aim at a better understanding of nonideal, dense, hot plasmas. This is due to the importance of understanding the evolution of planets and stars, whose cores consist of dense nonideal plasma [1]. Moreover, many expectations are associated with the use of plasma in inertial fusion reactors. Experimentally, dense nonideal plasmas are analyzed by the shock wave compression method [2], using high-power lasers [3] and ion accelerators [4]. A characteristic feature of the above-mentioned experiments is the nonisothermality of the resulting plasma. The reason for that is a great difference between ion and electron masses, which hampers the energy exchange between them. Therefore, the equilibrium inside ionic and electronic subsystems is reached much faster than that between ions and electrons [5]. To calculate the plasma properties correctly it is necessary to choose a model of interparticle interactions taking into account specific features and parameters of the system [6]. The subject of this paper is nonisothermal, weakly nonideal, dense plasmas. To describe such a type of plasma it is necessary to use a model of interparticle interactions taking into account collective and quantum effects.

The problem of calculating the equation of state for dense nonideal plasmas taking into account quantum effects was studied by a number of authors [7]. For example, Vorberger *et al.* [8,9] considered this problem using the Green's function method. In [10] quantum effects in dense plasmas were studied using quantum molecular dynamics. However, these models require a vast number of calculations. Therefore, to calculate the static properties of plasma in various fields of physics and astrophysics [11,12] it is necessary to have a simple analytical approach. Such a simple self-consistent analytical model, which can be used for the calculation of thermodynamic and structural characteristics of dense weakly coupled plasmas taking into account quantum effects, has been developed in this work.

It is known that two methods are used to determine the effective interparticle interaction potential taking into account the collective effects of charge screening at large distances. The first method is based on the solution to the generalized Poisson-Boltzmann equation obtained from Bogolyubov's equations for the phase-space distribution function [13–16]. The second method is based on the dielectric response function [17–21]. These effective potentials proved to be very useful in calculations of various plasma properties [22–31]. In this work the effective interaction potential is determined by the second method: the method of dielectric response function.

The dense plasma is a plasma where the average interparticle distance is comparable to the thermal de Broglie wavelength of particles. In dense plasmas, there is a high probability of interparticle collisions at very short distances, where it is important to consider the wave nature of the colliding particles caused by quantum-mechanical effects such as diffraction and symmetry. These effects at small distances can be taken into account in the pair interaction potential of particles or in the micro-potential [32–36]. Hence, at the first step we had to choose such a pair interaction potential between particles that would neglect the influence of the environment, satisfy the considered plasma parameters, and, as mentioned above, take into account the quantum effects of diffraction and symmetry at short distances. As a micropotential we used the Deutsch potential [32–34], which had been tested in a large number of calculations [37–40]

$$\phi_{\alpha\beta}^{\text{Deutsch}}(r) = \frac{Z_\alpha Z_\beta e^2}{r}\left(1 - \exp\left(-\frac{r}{\lambda_{\alpha\beta}}\right)\right), \tag{1}$$

where α and β are particle species (ion or electron); $Z_\alpha,\ Z_\alpha$ are atomic numbers of particle species α, β; e is the electron charge; $\lambda_{\alpha\beta} = \hbar/\sqrt{4\pi\ m_{\alpha\beta} k_B T_{\alpha\beta}}-$ is the thermal de-Broglie wavelength of pairs of particles α, β; $m_{\alpha\beta} = m_\alpha m_\beta/(m_\alpha + m_\beta)$ is the reduced mass and k_B is the Boltzmann constant; $T_{ee} = T_e$, $T_{ii} = T_i$ are the temperatures of the electron and ion subsystems. To describe the nonisothermal two-temperature plasma it is necessary to use not only temperatures of electrons and ions but also an electron-ion temperature T_{ei} [37,40]. In [40] the microscopic properties of the nonisothermal, nonideal plasma, particularly, in the long-wavelength limit of the static structure factor, were analyzed. Using the Ornstein-Zernike equation, it was shown that the electron-ion temperature should be expressed in terms of electron and ion temperatures in the following form:

$$T_{ei} = \sqrt{T_e T_i}. \tag{2}$$

Therefore, $T_{\alpha\beta} = \sqrt{T_\alpha T_\beta}$.

For the interaction between ions the thermal wavelength for an ion-ion pair should be taken as $\lambda_{ii} \to 0$ and the potential (1) for that pair is reduced to the Coulomb potential.

Using the potential (1), we will show that in the low density limit the well-known analytical results for the equation of state of plasmas, which were obtained from the general quantum statistical theory, can be reproduced. This indicates the correctness of the used potential (1). It should be noticed that the first quantum potential was obtained by Kelbg [41]. However, the Kelbg potential does not enable us to obtain analytical formulas for the effective screened interaction potential and thermodynamic characteristics of dense plasmas. A more detailed investigation of the correspondence between classical and quantum systems on the basis of quantum potentials may be found in [42].

As dimensionless plasma parameters, we use the coupling parameters Γ_{ee}, Γ_{ii}, Γ_{ei} and the density parameter r_S, which can be found from the following formulas:

$$\Gamma_{ee}=\frac{e^2}{ak_BT_e},\quad \Gamma_{ii}=\frac{{Z_i}^2e^2}{ak_BT_i}\left(\frac{n_i}{n_e}\right)^{1/3}=\Gamma_{ee}Z_i^{5/3}\left(\frac{T_e}{T_i}\right),$$
$$\Gamma_{ei}=\frac{Z_ie^2}{ak_BT_{ei}}=\Gamma_{ee}Z_i\sqrt{\frac{T_e}{T_i}},\quad r_S=a/a_B, \tag{3}$$

where $a=(3/(4\pi n_e))^{1/3}$ is the average distance between electrons. The ratio n_i/n_e is found from the semineutrality condition. Further, we will consider a fully ionized plasma with the following parameters: electron density varying from 10^{21} cm^{-3} to 10^{24} cm^{-3} and temperature varying from 10^4K to 10^6K. We assume that there is only one type of ion and $n_i/n_e=1/Z_i$.

II. EFFECTIVE INTERACTION POTENTIAL

As mentioned above, to obtain an analytical expression for the effective potential we used the method of dielectric response function, where the Deutsch potential was used as a micropotential (1). The Fourier transform of the effective potential is determined by the following formula:

$$\tilde{\Phi}_{\alpha\beta}(q)=\tilde{\varphi}_{\alpha\beta}(q)(\varepsilon(q))^{-1}, \tag{4}$$

where $\tilde{\phi}_{\alpha\beta}(q)$ is the Fourier transform of the interaction micropotential (1), $\varepsilon(q)$ is the dielectric function of the plasma in the random phase approximation, which is determined by the formula:

$$\varepsilon_{RPA}(q)=1+\sum_\alpha\frac{n_\alpha}{k_BT_\alpha}\tilde{\phi}_{\alpha\alpha}(q), \tag{5}$$

where n_α— is the density of α type of particles.

Using the inverse Fourier-transform formula we can obtain the expression for the effective interaction potential

$$\Phi_{\alpha\beta}(r)=\frac{Z_\alpha Z_\beta e^2}{r}\frac{1}{\gamma^2\sqrt{1-(2k_D/\lambda_{ee}\gamma^2)^2}}\left(\left(\frac{1/\lambda_{ee}^2-B^2}{1-B^2\lambda_{\alpha\beta}^2}\right)\exp(-Br)-\left(\frac{1/\lambda_{ee}^2-A^2}{1-A^2\lambda_{\alpha\beta}^2}\right)\exp(-Ar)\right)$$
$$-\frac{Z_\alpha Z_\beta e^2}{r}\frac{(1-\delta_{\alpha\beta})}{1+C_{\alpha\beta}}\exp(-r/\lambda_{\alpha\beta}), \tag{6}$$

where $(2k_D/\lambda_{ee}\gamma^2)^2<1$, $k_D^2=k_e^2+k_i^2$ is the screening parameter taking into account the contribution of electrons and ions, $\gamma^2=k_i^2+1/\lambda_{ee}^2$, and

$$C_{\alpha\beta}=\frac{k_D^2\lambda_{\alpha\beta}^2-k_i^2\lambda_{ee}^2}{\lambda_{ee}^2/\lambda_{\alpha\beta}^2-1},\quad A^2=\frac{\gamma^2}{2}\left(1+\sqrt{1-\left(\frac{2k_D}{\lambda_{ee}\gamma^2}\right)^2}\right),\quad B^2=\frac{\gamma^2}{2}\left(1-\sqrt{1-\left(\frac{2k_D}{\lambda_{ee}\gamma^2}\right)^2}\right). \tag{7}$$

The effective potential (6) describes the interaction between all pairs of particles. In the last term on the right-hand side of the equation, the symbol $1-\delta_{\alpha\beta}$ was included formally to indicate that this term disappears for ion-ion and electron-electron interaction. The symbol $1-\delta_{\alpha\beta}$ can be neglected, as for ion-ion case $\lambda_{ii}\to 0$ and the term $\exp(-r/\lambda_{\alpha\beta})$ tends to zero, for the electron-electron case according to Eq. (11) $C_{ee}\to\infty$ and the last term on the right-hand side of the equation tends to zero. Thus, the symbol $1-\delta_{\alpha\beta}$ enables us not to make transformations every time we consider ion-ion or electron-electron pairs.

From (6) we can obtain the analytical expressions for effective electron-electron interaction potential

$$\Phi_{ee}(r)=\frac{e^2}{(1+\lambda_{ee}^2k_i^2)\sqrt{1-(2k_D/\lambda_{ee}\gamma^2)^2}}\frac{(\exp(-Br)-\exp(-Ar))}{r}, \tag{8}$$

for the effective ion-ion interaction potential

$$\Phi_{ii}(r)=\frac{Z_iZ_ie^2}{\gamma^2\sqrt{1-(2k_D/\lambda_{ee}\gamma^2)^2}\,r}\left(\exp(-Br)\left(\frac{1}{\lambda_{ee}^2}-B^2\right)-\exp(-Ar)\left(\frac{1}{\lambda_{ee}^2}-A^2\right)\right), \tag{9}$$

and for the effective electron-ion interaction potential

$$\Phi_{ei}(r)=-\frac{Z_ie^2}{\lambda_{ei}^2\gamma^2\sqrt{1-(2k_D/\lambda_{ee}\gamma^2)^2}\,r}\left(\left(\frac{1/\lambda_{ee}^2-B^2}{1/\lambda_{ei}^2-B^2}\right)\exp(-Br)-\left(\frac{1/\lambda_{ee}^2-A^2}{1/\lambda_{ei}^2-A^2}\right)\exp(-Ar)\right)+\frac{e^2}{r}\frac{1}{1+C_{ei}}\exp(-r/\lambda_{ei}). \tag{10}$$

The effective potentials satisfy all passages to the limit. If there is no screening $k_D \to 0, k_i \to 0, k_e \to 0$, formulas (8), (9), and (10) can be written as

$$\Phi_{ee}(r) = \frac{e^2}{r}(1 - \exp(-r/\lambda_{ee})), \tag{11}$$

$$\Phi_{ii}(r) = \frac{Z_i Z_i e^2}{r}, \tag{12}$$

$$\Phi_{ei}(r) = -\frac{Z_i e^2}{r}(1 - \exp(-r/\lambda_{ei})), \tag{13}$$

which coincides with the micropotentials used as initial potentials. When $\lambda_{ee} \to 0, \lambda_{ei} \to 0$ the expression for the effective potential (6) transforms into the formula for the Debye screened potential without quantum effects

$$\Phi_{\alpha\beta}(r) = \frac{Z_\alpha Z_\beta e^2}{r}\exp(-r k_D). \tag{14}$$

In the case $k_i \to 0$ the effective potential (8) coincides with the potential obtained in [18,32], and the effective potential (9) coincides with the effective potential for ion interactions derived in [19]. These effective potentials were used to study various properties of plasmas [24–31,43–47].

If the term $(2k_D/\lambda_{ee}\gamma^2)^2$ is greater than one in (6), the square root term becomes imaginary. As the effective interaction potential (6) is always real, in the case of $(2k_D/\lambda_{ee}\gamma^2)^2 > 1$ it is convenient to use the formula (6) in a modified form without the imaginary unit

$$\sqrt{1 - (2k_D/\lambda_{ee}\gamma^2)^2} = \sqrt{-1}\sqrt{(2k_D/\lambda_{ee}\gamma^2)^2 - 1}.$$

In this case, it is easy to show that the effective potential (6) takes the following form:

$$\begin{aligned}\Phi_{\alpha\beta}(r) = {} & \frac{Z_\alpha Z_\beta e^2}{r}\frac{d_{\alpha\beta}}{\gamma^2\sqrt{(2k_D/\lambda_{ee}\gamma^2)^2 - 1}}\sin\left(\sqrt{k_D/\lambda_{ee}}\sin(\omega/2)\, r + \theta_{\alpha\beta}\right)\exp\left[-r\sqrt{k_D/\lambda_{ee}}\cos(\omega/2)\right] \\ & - \frac{Z_\alpha Z_\beta e^2}{r}\frac{(1-\delta_{\alpha\beta})}{1 + C_{\alpha\beta}}\exp(-r/\lambda_{\alpha\beta}),\end{aligned} \tag{15}$$

where $(2k_D/\lambda_{ee}\gamma^2)^2 > 1$ and the constants $d_{\alpha\beta}, \theta_{\alpha\beta}, \omega$ are defined as

$$d_{\alpha\beta} = \sqrt{a_{\alpha\beta}^2 + b_{\alpha\beta}^2}, \quad \theta_{\alpha\beta} = \arctan(b_{\alpha\beta}/a_{\alpha\beta}), \quad \omega = \arctan\left[\sqrt{(2k_D/\lambda_{ee}\gamma^2)^2 - 1}\right],$$

$$a_{\alpha\beta} = \frac{2(1/\lambda_{ee}^2 - \gamma^2/2)(1 - \gamma^2\lambda_{\alpha\beta}^2/2) + \gamma^4\lambda_{\alpha\beta}^2((2k_D/\lambda_{ee}\gamma^2)^2 - 1)}{(1 - \gamma^2\lambda_{\alpha\beta}^2/2)^2 + \gamma^4\lambda_{\alpha\beta}^4(4{k_D}^2/{\lambda_{ee}}^2\gamma^4 - 1)/4},$$

$$b_{\alpha\beta} = \frac{\gamma^2(1 - \lambda_{\alpha\beta}^2/\lambda_{ee}^2)\sqrt{(2k_D/\lambda_{ee}\gamma^2)^2 - 1}}{(1 - \gamma^2\lambda_{\alpha\beta}^2/2)^2 + \gamma^4\lambda_{\alpha\beta}^4(4{k_D}^2/{\lambda_{ee}}^2\gamma^4 - 1)/4}.$$

It should be noticed that the same result obtained if an imaginary unit, first, is removed from (4) taking into account the condition $(2k_D/\lambda_{ee}\gamma^2)^2 > 1$ and only then the inverse Fourier transformation performed. We refer to [48] where the similar mathematical procedure was used.

Figures 1–4 show the effective potentials (6) and (15) in comparison with the Deutsch (1) and Debye potentials for different types of interactions, where $\Gamma_{ee} = \Gamma_{ii} = \Gamma_{ei} = \Gamma$. It can be seen from the figures that, due to the collective effects and the wave nature of electrons, the effective potentials for the electron-electron and electron-ion interactions are screened at large distances and finite at small distances. The effective ion-ion interaction potential is also screened at large distances, but, as a consequence, due to the wave nature of electrons, the screening is slightly weaker than the Debye potential.

The effective interaction potentials (6) and (15) can be used to describe multicomponent dense weakly coupled two-temperature plasmas with parameters of nonideality less than unity $\Gamma_{ii} < 1, \Gamma_{ee} < 1$. In the case where the ion subsystem is strongly coupled $\Gamma_{ii} > 1$, and the electron subsystem is weakly nonideal $\Gamma_{ee} < 1$ or ideal $\Gamma_{ee} \ll 1$, then $k_i = 0$ and the effective potentials (8) and (15) ($\alpha = i, \beta = i$) can be used to study the strongly coupled one-component ion plasma with a background of quasiclassical weakly coupled electrons. In this case, the effective ion interaction potential is expressed as

$$\begin{aligned}\Phi_{ii}(r) & \\ = {} & \frac{Z_i^2 e^2}{r\sqrt{1 - (2\lambda_{ee}k_e)^2}}\left(\left(\frac{1}{2} + \frac{1}{2}\sqrt{1 - (2\lambda_{ee}k_e)^2}\right)\right. \\ & \left.\times\exp(-Br) - \left(\frac{1}{2} - \frac{1}{2}\sqrt{1 - (2\lambda_{ee}k_e)^2}\right)\exp(-Ar)\right),\end{aligned} \tag{16}$$

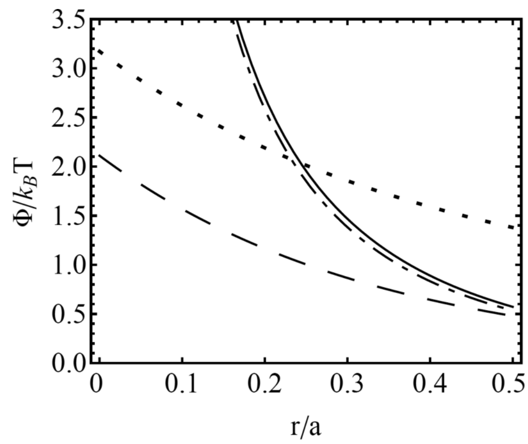

FIG. 1. Interaction potentials at $\Gamma = 0.8$, $r_S = 2$: Solid line corresponds to (9) for $i-i$ pairs; Dashed-dotted line is the Debye potential; Dashed line—Eq. (8); Dotted line micropotential (1).

for $(2k_e\lambda_{ee})^2 < 1$ and

$$\Phi_{ii}(r) = \frac{Z_i^2 e^2}{r} \frac{2k_e\lambda_{ee}}{\sqrt{(2\lambda_{ee}k_e)^2 - 1}} \sin(\sqrt{k_e/\lambda_{ee}} \sin(\omega/2)\, r + \theta_{ii}) \times \exp[-r\sqrt{k_e/\lambda_{ee}} \cos(\omega/2)], \quad (17)$$

for $(2k_e\lambda_{ee})^2 > 1$.

The constant coefficients in formulas (16) and (17) read

$$B^2 = \frac{1}{2\lambda_{ee}^2}\left(1 - \sqrt{1 - 4\lambda_{ee}^2 k_e^2}\right),$$

$$A^2 = \frac{1}{2\lambda_{ee}^2}\left(1 + \sqrt{1 - 4\lambda_{ee}^2 k_e^2}\right),$$

$$\omega = \theta_{ii} = \arctan\left(\sqrt{4\lambda_{ee}^2 k_e^2 - 1}\right).$$

Thus, the effective potentials (16) and (17) can be used molecular dynamics and Monte Carlo simulations or for the calculation of the stopping power of plasmas with a strongly nonideal ion component for $\Gamma_{ee} < 1$.

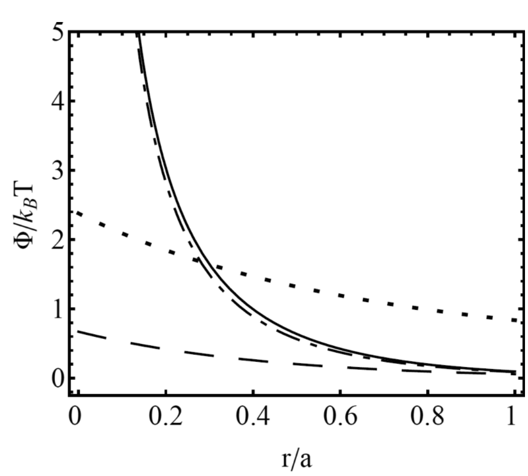

FIG. 2. Interaction potentials at $\Gamma = 0.9$, $r_S = 1$: Solid line corresponds to (15) for $i-i$ pairs; Dashed-dotted line, the Debye potential; Dashed line—Eq. (15) for $e-e$ pair; Dotted line—micropotential (1).

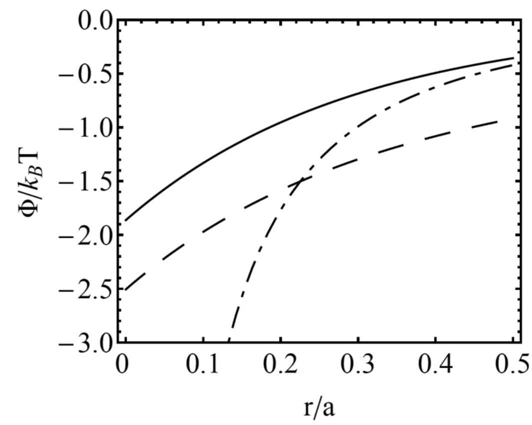

FIG. 3. Effective potentials of interaction between electrons and ions at $\Gamma = 0.8$, $r_S = 2$: Solid line—Eq. (10); Dashed-dotted line-the Debye potential; Dashed line, micropotential (1).

It should be noted that (16) and (17) describe the same effective interaction potential [the same applies to (6) and (15)]. The potential (16) transforms into (17) by replacing $\sqrt{1 - 4\lambda_{ee}^2 k_e^2} = i\sqrt{4\lambda_{ee}^2 k_e^2 - 1}$ and vice versa. In the case $4\lambda_{ee}^2 k_e^2 = 1$, (16) and (17) take the same simple form

$$\Phi_{ii}(r) = \frac{Z_i^2 e^2}{r}\left(1 + \frac{r}{2\sqrt{2}\lambda_{ee}}\right)\exp\left(-\frac{r}{\sqrt{2}\lambda_{ee}}\right). \quad (18)$$

Using dimensionless parameters, the condition $4\lambda_{ee}^2 k_e^2 = 1$ can be rewritten as $\Gamma_{ee} = \sqrt{\pi\ r_S/6}$.

The effective potentials (17) and (18) and the Debye potential $\phi_D = Z_i^2 \exp(-r\,k_e)/r$ are shown in Figs. 5 and 6. As can be seen, the effect of screening is weaker due to quantum effects.

The effective potential of ion-ion interaction (17), obtained in the quasiclassical approximation, gives a negative minimum (Fig. 7), i.e., the attraction between ions for certain plasma parameters. A similar result was obtained in [48] in the framework of the generalized quantum hydrodynamics approximation and was considered in detail using the density functional theory in [49–51].

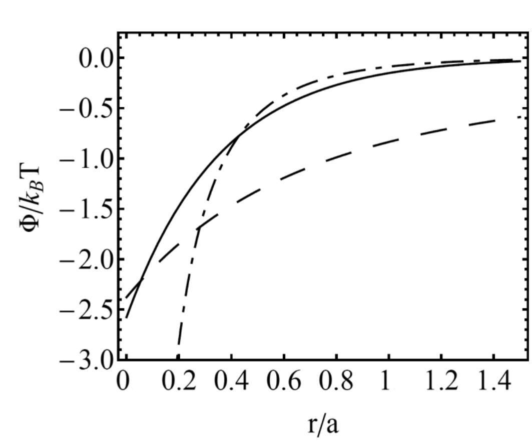

FIG. 4. Effective potentials of interaction between electrons and ions at $\Gamma = 0.9$, $r_S = 1$: Solid line—Eq. (15); Dashed-dotted line-the Debye potential; Dashed line-micropotential (1).

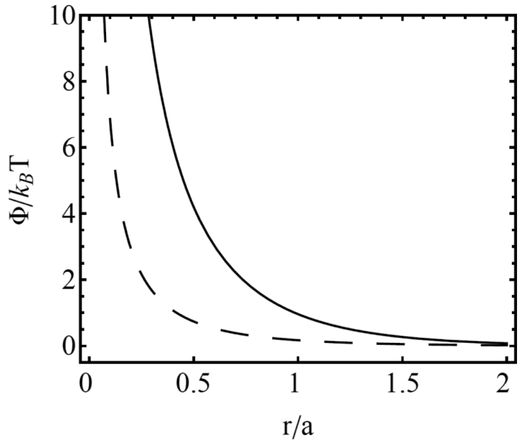

FIG. 5. Effective potentials of ion interaction at $\Gamma_{ii} = 4$, $\Gamma_{ee} = 0.8$, $r_S = 1$: Solid line—Eq. (17); Dashed line—the Debye potential.

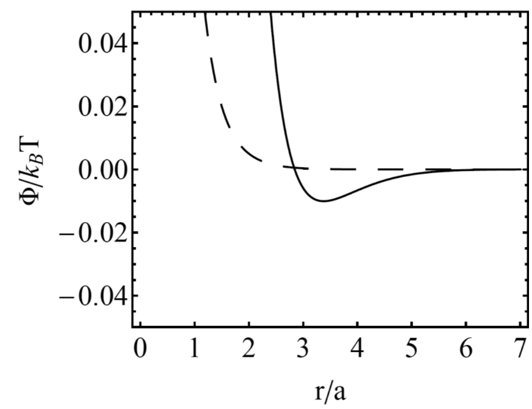

FIG. 7. Effective interaction potentials for $\Gamma_{ii} = 10$, $\Gamma_{ee} = 0.8$, $r_S = 0.4$: Solid line—the effective potential of ion interaction, Eq. (17); Dashed line—the Debye potential.

III. DENSE PLASMA THERMODYNAMIC PROPERTIES

The resulting effective screened potentials enable us to study various plasma properties directly. To study the thermodynamic properties of the plasma we used a method using particle pair correlation functions $g_{\alpha\beta}(r)$. For weakly ionized plasma

$$g_{\alpha\beta}(r) = \exp\left(-\frac{\Phi_{\alpha\beta}(r)}{k_B T_{\alpha\beta}}\right) \approx 1 - \frac{\Phi_{\alpha\beta}(r)}{k_B T_{\alpha\beta}}.$$

Obviously, the behavior of the pair correlation function is explained by the behavior of the effective interaction potential. The graphs of the pair correlation function and the structure factor with their description are given in Appendix. Further we will show analytical formulas for the interaction correlation energy and for the equation of state for a fully ionized plasma.

A. Interaction correlation energy

The total internal energy of a plasma is equal to $U = \sum_\alpha 3/2 N_\alpha k_B T_\alpha + U_N$ where the correlation energy of interaction is determined by the formula

$$U_N = 2\pi V \int_0^\infty \sum_{\alpha,\beta} n_\alpha, n_\beta \varphi_{\alpha\beta}(r) g_{\alpha\beta}(r) r^2 dr. \quad (19)$$

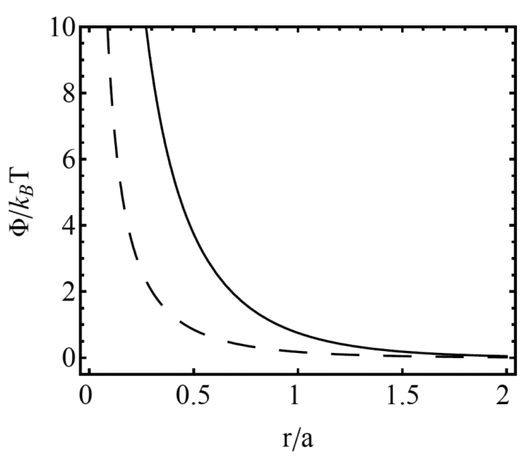

FIG. 6. Effective potentials of ion interaction at $\Gamma_{ii} = 4$, $r_S = 2$, $\Gamma_{ee} = \sqrt{\pi\, r_S/6}$: Solid line—Eq. (18); Dashed line—the Debye potential.

Taking the Deutsch potential (1) as the interaction micropotential $\varphi_{\alpha\beta}(r)$ and using the obtained effective screened interaction potentials (6) to define the pair-correlation function, we obtained the analytical expression for the correlation energy for $(2k_D/\lambda_{ee}\gamma^2)^2 \leqslant 1$:

$$\begin{aligned} U_N = &-2\pi V \sum_{\alpha,\beta} \frac{n_\alpha, n_\beta\, e_\alpha^2 e_\beta^2}{k_B T_{\alpha\beta}\gamma^2\sqrt{1-(2k_D/\lambda_{ee}\gamma^2)^2}} \\ &\times \left[\frac{1/\lambda_{ee}^2 - B^2}{B\left(1-B^2\lambda_{\alpha\beta}^2\right)(1+B\lambda_{\alpha\beta})} \right. \\ &\left. - \frac{1/\lambda_{ee}^2 - A^2}{A\left(1-A^2\lambda_{\alpha\beta}^2\right)(1+A\lambda_{\alpha\beta})}\right] \\ &+ 2\pi V e^2\left(2Z_i n_i n_e \lambda_{ei}^2 - n_e^2\lambda_{ee}^2 + \frac{Z_i n_i n_e \lambda_{ei} e^2}{k_B T_{ei}(1-C_{ei})}\right). \end{aligned} \quad (20)$$

The second term in (20) appears due to the quantum diffraction effect at small distances. Let us denote it by $U_{\rm dif}$ and the first term by $U_{\rm long}$. If the wavelength of particles tends to zero, $U_{\rm dif}$ term vanishes, and $U_{\rm long}$ gives the well-known Debye correction. Formula (20) is consistent with the results of [33] for the one-component electron plasma. The first term $U_{\rm dif}$ are proportional to $\sim T^{-1}\hbar^2$ and second term is proportional to $\sim T^{-3/2}\hbar$.

To account for the effect of symmetry it is necessary to add a symmetrical member, taking into account the additional effective repulsion between the electrons due to the Pauli exclusion principle [32], into the Deutsch micropotential and into the effective potential (6)

$$\varphi_S(r) = \delta_{\alpha e}\delta_{\beta e} k_B T_e \ln 2 \exp\left(-\frac{\ln 2}{\pi}\left(\frac{r}{\lambda_{ee}}\right)^2\right), \quad (21)$$

where $\delta_{\alpha e}$, $\delta_{\beta e}$ are Kronecker symbols.

When taking into account the effect of symmetry, there is an additional term in the correlation energy

$$U_{\rm sym} = 2\pi V n_e^2 \frac{e^2\pi^2\lambda_{ee}^3}{4\sqrt{\ln 2}\left(1+\lambda_{ee}^2 k_i^2\right)\sqrt{1-\left(2k_D/\lambda_{ee}\gamma^2\right)^2}}\left[B\exp\left(\frac{\pi^2 B^2\lambda_{ee}^2}{4\ln 2}\right)\mathrm{erfc}\left(\frac{\sqrt{\pi}B\lambda_{ee}}{2\sqrt{\ln 2}}\right)\right.$$
$$\left.-A\exp\left(\frac{\pi^2 A^2\lambda_{ee}^2}{4\ln 2}\right)\mathrm{erfc}\left(\frac{\sqrt{\pi}A\lambda_{ee}}{2\sqrt{\ln 2}}\right)\right] - 2\pi V n_e^2\left(1.21685 e^2\lambda_{ee}^2\right) + 2\pi V n_e^2\left(1.9828 k_B T_e\lambda_{ee}^3\right). \quad (22)$$

Thus, the correlation energy is the sum of expressions (20) and (22).

If $(2k_D/\lambda_{ee}\gamma^2)^2 < 1$ is not fulfilled, it is necessary to use the effective potential (15). For the correlation energy, excluding the effect of symmetry from Eq. (19), we find

$$U_N = -2\pi V\sum_{\alpha,\beta}\frac{n_\alpha n_\beta e_\alpha^2 e_\beta^2 d_{\alpha\beta}}{k_B T_{\alpha\beta}\gamma^2\sqrt{\left(2k_D/\lambda_{ee}\gamma^2\right)^2-1}}\left[\sqrt{\frac{\lambda_{ee}}{k_D}}\sin\left(\frac{\omega}{2}+\theta_{\alpha\beta}\right) - \frac{\lambda_{\alpha\beta}^2\sqrt{\frac{k_D}{\lambda_{ee}}}\sin\left(\frac{\omega}{2}+\theta_{\alpha\beta}\right)+\lambda_{\alpha\beta}\sin\left(\frac{\omega}{2}\right)}{\lambda_{\alpha\beta}^2\frac{k_D}{\lambda_{ee}}+2\lambda_{\alpha\beta}\sqrt{\frac{k_D}{\lambda_{ee}}}\cos\left(\frac{\omega}{2}\right)+1}\right]$$
$$+2\pi V e^2\left(2Z_i n_i n_e\lambda_{ei}^2 - n_e^2\lambda_{ee}^2 + \frac{Z_i n_i n_e\lambda_{ei}e^2}{k_B T_{ei}(1-C_{ei})}\right), \quad (23)$$

where $(2k_D/\lambda_{ee}\gamma^2)^2 > 1$.

Including the symmetry effect we get the following contribution to the correlation energy:

$$U_{\rm sym} = 2\pi V n_e^2\frac{e^2\pi^2\lambda_{ee}^3\sqrt{k_D/\lambda_{ee}}}{4\sqrt{\ln 2}\left(1+\lambda_{ee}^2k_i^2\right)\sqrt{\left(2k_D/\lambda_{ee}\gamma^2\right)^2-1}}\exp\left(-\frac{\pi}{4\ln 2}k_D\lambda_{ee}\cos(\omega)\right)\left\{\cos\left(\frac{\omega}{2}-\frac{\pi k_D\lambda_{ee}}{4\ln 2}\right)\right.$$
$$\left.\times\,\mathrm{Im}\left(\mathrm{erf}\left(\frac{1}{2}\sqrt{\frac{\pi k_D\lambda_{ee}}{\ln 2}}\exp\left(\frac{i\omega}{2}\right)\right)\right) - \sin\left(\frac{\omega}{2}-\frac{\pi k_D\lambda_{ee}}{4\ln 2}\right)\left[1-\mathrm{Re}\left(\mathrm{erf}\left(\frac{1}{2}\sqrt{\frac{\pi k_D\lambda_{ee}}{\ln 2}}\exp\left(\frac{i\omega}{2}\right)\right)\right)\right]\right\}$$
$$-2\pi V n_e^2\left(1.21685\times e^2\lambda_{ee}^2\right)+2\pi V n_e^2\left(1.9828\times k_B T_e\lambda_{ee}^3\right). \quad (24)$$

For $(2k_D/\lambda_{ee}\gamma^2)^2 > 1$ the correlation energy is the sum of (23) and (24).

The first two terms in (22) and (24) for isothermal plasma are proportional to $\sim T^{-1}\hbar^2$ and the third term is proportional to $\sim T^{-1/2}\hbar^3$. It means that symmetry effects give only a small contribution to the plasma correlation energy.

All expressions for the internal energy, regardless of the sign of the radicand $\sqrt{1-4\lambda_{ee}^2k_e^2}$, are always real. Formulas (23), (24) can be obtained by replacing $\sqrt{1-4\lambda_{ee}^2k_e^2} = i\sqrt{4\lambda_{ee}^2k_e^2-1}$ in expressions (20) and (22), respectively. Figures 8 and 9 show a comparison of the internal energy to the results of other studies, obtained by theoretical methods and by computer simulation [23,52–55]. Figure 9 shows that the obtained analytical expression for the correlation energy coincides with the Debye correction for small values of the coupling parameter. A slight difference between our internal energy and the results of [23,52] for large values of the coupling parameter, can be explained by the appearance of bound states (neutral atoms), which were not considered in this paper.

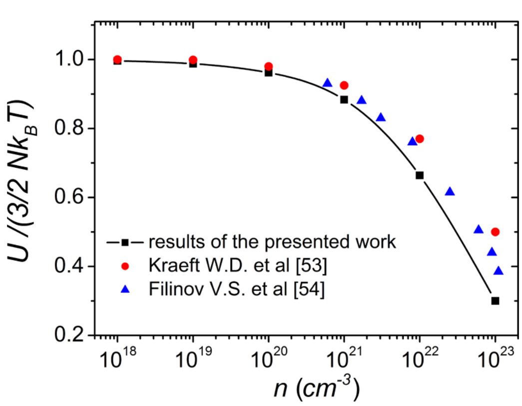

FIG. 8. (Color online) Internal energy of isothermal hydrogen plasma at $T = 125\,000$ K.

B. Plasma equation of state

The plasma equation of state is written as

$$P = P_{id} - \frac{2\pi}{3}\int_0^\infty\sum_{\alpha,\beta}n_\alpha,n_\beta\frac{d\varphi_{\alpha\beta}(r)}{dr}g_{\alpha\beta}(r)r^3dr, \quad (25)$$

where $P_{id} = n_e k_B T_e + n_i k_B T_i$ is the pressure of ideal plasma.

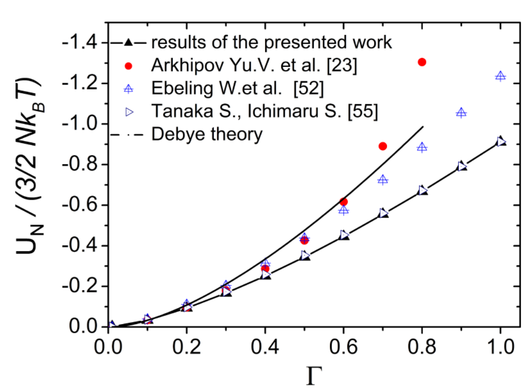

FIG. 9. (Color online) Correlation energy of a hydrogen plasma.

As in the case of the correlation energy, taking the Deutsch potential (1) as the interaction micropotential $\varphi_{\alpha\beta}(r)$ and using the effective screened potentials without the diffraction effect, we obtain the following analytical expression for the equation of state:

$$P = P_{id} - \frac{2\pi}{3}\sum_{\alpha,\beta}\frac{n_\alpha n_\beta e_\alpha^2 e_\beta^2}{k_B T_{\alpha\beta}\gamma^2\sqrt{1-(2k_D/\lambda_{ee}\gamma^2)^2}}\left[\frac{1/\lambda_{ee}^2 - B^2}{B(1-B^2\lambda_{\alpha\beta}^2)(1+B\lambda_{\alpha\beta})^2} - \frac{1/\lambda_{ee}^2 - A^2}{A(1-A^2\lambda_{\alpha\beta}^2)(1+A\lambda_{\alpha\beta})^2}\right]$$
$$+ 2\pi e^2\left(2Z_i n_i n_e \lambda_{ei}^2 - n_e^2\lambda_{ee}^2 + \frac{Z_i n_i n_e \lambda_{ei} e^2}{12 k_B T_{ei}(1-C_{ei})}\right). \tag{26}$$

where $(2k_D/\lambda_{ee}\gamma^2)^2 \leqslant 1$.

Formula (26) also reproduces the results for the equation of state for a single-component electron plasma derived in [33]. When the thermal wavelength of particles tends to zero, the last term in (26) disappears and the Debye correction remains. Taking into account the effect of symmetry, we get the following additional terms in the analytical expression for the equation of state:

$$P_{\rm sym} = \frac{2\pi}{3}\frac{e^2\pi^2 n_e^2\lambda_{ee}^4}{4\ln 2(1+\lambda_{ee}^2 k_i^2)\sqrt{1-(2k_D/\lambda_{ee}\gamma^2)^2}}\left[\gamma^2\sqrt{1-(2k_D/\lambda_{ee}\gamma^2)^2} + \frac{\pi\lambda_{ee}}{2\sqrt{\ln 2}}B\left(B^2 + \frac{6\ln 2}{\pi\lambda_{ee}^2}\right)\right.$$
$$\left.\times \exp\left(\frac{\pi^2 B^2\lambda_{ee}^2}{4\ln 2}\right)\mathrm{erfc}\left(\frac{\sqrt{\pi}B\lambda_{ee}}{2\sqrt{\ln 2}}\right) - \frac{\pi\lambda_{ee}}{2\sqrt{\ln 2}}A\left(A^2 + \frac{6\ln 2}{\pi\lambda_{ee}^2}\right)\exp\left(\frac{\pi^2 A^2\lambda_{ee}^2}{4\ln 2}\right)\mathrm{erfc}\left(\frac{\sqrt{\pi}A\lambda_{ee}}{2\sqrt{\ln 2}}\right)\right]$$
$$+ \frac{2\pi}{3}n_e^2(0.618504\times e^2\lambda_{ee}^2) + \frac{2\pi}{3}n_e^2(2.4833\times k_B T_e\lambda_{ee}^3). \tag{27}$$

If $(2k_D/\lambda_{ee}\gamma^2)^2 > 1$, the equation of state without the symmetry effect is written as

$$P = P_{id} - \frac{2\pi}{3}\sum_{\alpha,\beta}\frac{n_\alpha n_\beta e_\alpha^2 e_\beta^2 d_{\alpha\beta}}{k_B T_{\alpha\beta}\gamma^2\sqrt{(2k_D/\lambda_{ee}\gamma^2)^2-1}}\left[-\sqrt{\frac{\lambda_{ee}}{k_D}}\sin\left(\frac{\omega}{2}+\theta_{\alpha\beta}\right) + \frac{\lambda_{\alpha\beta}^2\sqrt{\frac{k_D}{\lambda_{ee}}}\sin\left(\frac{\omega}{2}+\theta_{\alpha\beta}\right) + \lambda_{\alpha\beta}\sin\left(\frac{\omega}{2}\right)}{\lambda_{\alpha\beta}^2\frac{k_D}{\lambda_{ee}} + 2\lambda_{\alpha\beta}\sqrt{\frac{k_D}{\lambda_{ee}}}\cos\left(\frac{\omega}{2}\right)+1}\right.$$
$$\left.+\frac{\lambda_{\alpha\beta}\sin\left(\theta_{\alpha\beta} + 2\arctan\left(\frac{\sqrt{k_D/\lambda_{ee}}\sin(\omega/2)}{\sqrt{k_D/\lambda_{ee}}\cos(\omega/2)+\lambda_{\alpha\beta}^{-1}}\right)\right)}{\lambda_{\alpha\beta}^2\frac{k_D}{\lambda_{ee}} + 2\lambda_{\alpha\beta}\sqrt{\frac{k_D}{\lambda_{ee}}}\cos\left(\frac{\omega}{2}\right)+1}\right] + 2\pi e^2\left(2Z_i n_i n_e\lambda_{ei}^2 - n_e^2\lambda_{ee}^2 + \frac{Z_i n_i n_e\lambda_{ei}e^2}{12k_B T_{ei}(1-C_{ei})}\right). \tag{28}$$

If the effect of symmetry is taken into account, the following additional term appears:

$$P_{\rm sym} = \frac{2\pi}{3}n_e^2(0.618504\times e^2\lambda_{ee}^2) + \frac{2\pi}{3}n_e^2(2.4833\times k_B T_e\lambda_{ee}^3)$$
$$+ \frac{e^2\pi^2 n_e^2\lambda_{ee}^2}{2(1+\lambda_{ee}^2k_i^2)\sqrt{(2k_D/\lambda_{ee}\gamma^2)^2-1}}\int_0^\infty t\exp\left(-t\,\frac{\lambda_{ee}k_D}{4\ln 2}\cos(\omega)\right)\sin\left(t\,\frac{\lambda_{ee}k_D}{4\ln 2}\sin(\omega)\right)(1+t)^{-5/2}dt. \tag{29}$$

All terms in (27) and (29) are proportional to various degrees of the Plank constant, from 2 and higher. It is seen that expressions (27) and (29) give positive contributions to the pressure, which can be explained by the fact that the effect of quantum symmetry generates an effective repulsion between particles.

As in the case of the formulas for the correlation energy, (28) and (29) can be obtained from (26) and (27) by directly replacing $\sqrt{1-4\lambda_{ee}^2k_e^2} = i\sqrt{4\lambda_{ee}^2k_e^2-1}$.

Figures 10 and 11 show the comparison with the results of other works obtained by theoretical methods and by computer simulation [56–60]. The figures show good agreement with the results of molecular dynamics simulations based on wave packets [56] and with the results of Monte Carlo simulation based on path integrals [57,58]. The difference at high densities is due to the appearance of bound states, which were not taken into account in this paper.

Let us consider the low density limit. Neglecting the terms proportional to $\sim\lambda_{ee}^2/r_D^2$ in (26), in addition to the Debye correction for the excess part of the equation of state, we obtained the term $-k_B T_e\lambda_{ee}/(24\pi r_D^4)$. This result agrees with the Montroll-Ward contribution and corresponds to the quantum ring sum [61,62]. Therefore we can conclude that the derived equation of state for plasma has the correct asymptotic.

C. Thermodynamic properties on the basis of the Coulomb potential

Here, taking the Coulomb potential as the interaction micropotential $\varphi_{\alpha\beta}(r)$ and using the obtained effective screened interaction potentials (6) to determine the pair-correlation function, we obtained an analytical expression for the correlation energy and the equation of state. The analytical expression

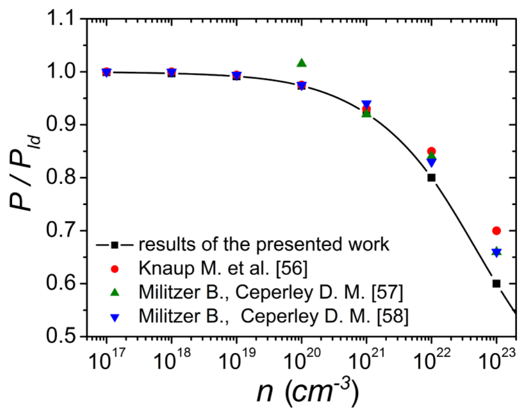

FIG. 10. (Color online) Equation of state for a hydrogen plasma at $T = 100\,000$ K.

for the correlation energy was written as

$$U_N = -2\pi V \sum_{\alpha,\beta} \frac{n_\alpha, n_\beta\, e_\alpha^2 e_\beta^2}{k_B T_{\alpha\beta}\gamma^2\sqrt{1-(2k_D/\lambda_{ee}\gamma^2)^2}} \times \left[\frac{1/\lambda_{ee}^2 - B^2}{B\left(1-B^2\lambda_{\alpha\beta}^2\right)} - \frac{1/\lambda_{ee}^2 - A^2}{A\left(1-A^2\lambda_{\alpha\beta}^2\right)}\right] + 2\pi V \frac{Z_i n_i n_e \lambda_{ei} e^4}{k_B T_{ei}(1-C_{ei})} + U_{\mathrm{sym}}, \tag{30}$$

where U_{sym} is the term due to the effect of symmetry

$$U_{\mathrm{sym}} = -2\pi V n e^4\left(1.2168 \times \lambda_{ee}^2\right). \tag{31}$$

The analytical expression for the equation of state can be written in the following form:

$$P = P_{id} - \frac{2\pi}{3} \sum_{\alpha,\beta} \frac{n_\alpha, n_\beta\, e_\alpha^2 e_\beta^2}{k_B T_{\alpha\beta}\gamma^2\sqrt{1-(2k_D/\lambda_{ee}\gamma^2)^2}} \times \left[\frac{1/\lambda_{ee}^2 - B^2}{B\left(1-B^2\lambda_{\alpha\beta}^2\right)} - \frac{1/\lambda_{ee}^2 - A^2}{A\left(1-A^2\lambda_{\alpha\beta}^2\right)}\right] + \frac{2\pi}{3}\frac{Z_i n_i n_e \lambda_{ei} e^4}{k_B T_{ei}(1-C_{ei})} + P_{\mathrm{sym}}, \tag{32}$$

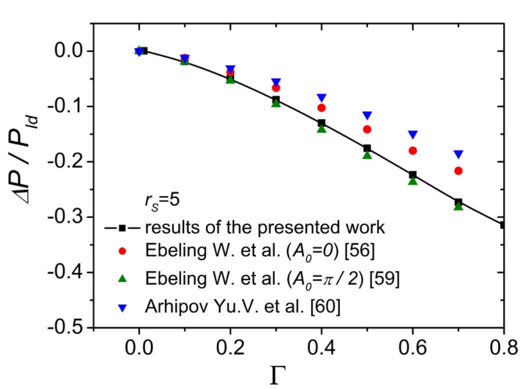

FIG. 11. (Color online) Excess part of equation of state for a hydrogen plasma.

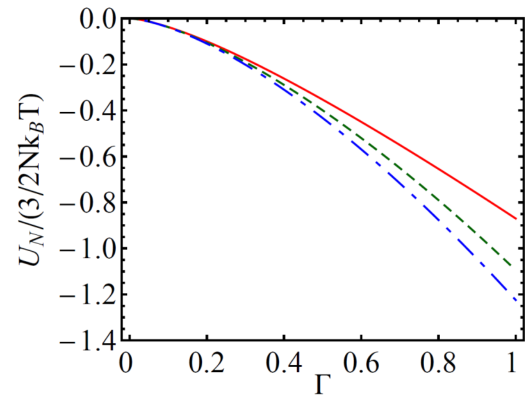

FIG. 12. (Color online) Correlation energy of isothermal hydrogen plasma at $r_s = 3$. Solid line corresponds to the results of Sec. III A, dashed line is obtained according to (30), dashed-dotted line presents results of the Debye theory.

where P_{sym} is the term due to the effect of symmetry

$$P_{\mathrm{sym}} = -\frac{\pi^2}{3} n_e^2 e^2 \lambda_{ee}^2. \tag{33}$$

Neglecting the terms proportional to $\sim\lambda_{ee}^2/r_D^2$ in (32), we have obtained that in the low density limit there is no term corresponding to the quantum ring sum (the Montroll-Ward contribution). Figures 12 and 13 show that the main quantum contribution is caused by the quantum ring sum proportional to $\sim\lambda_{ee}/r_D$. More clearly, it is seen in Fig. 13. The quantum effect causes a decrease in the correction due to nonideality in both the correlation energy and the excess part of the equation of state. The comparison with the result of Rieman *et al.* [63], which was obtained within a perturbation expansion using the thermodynamic Green's function, shows that the equation of state derived in Sec. IIIB is correct in the limit of weak coupling. Moreover, as it is seen from comparison with the results of the path integral Monte Carlo calculations by

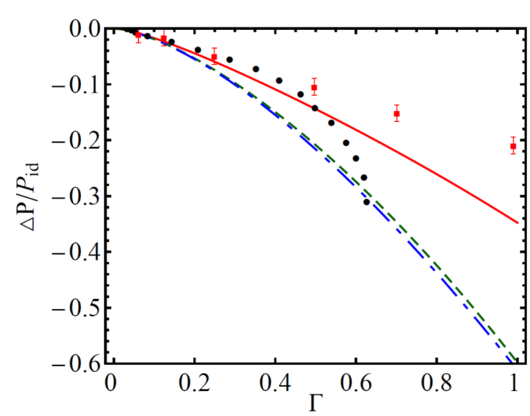

FIG. 13. (Color online) Excess part of equation of state for hydrogen plasma at $r_s = 1$. The solid line corresponds to the results of Sec. III B, the dashed line is obtained according to (32), the dashed-dotted line presents results of the Debye correction. Circles correspond to the results of Riemann *et al.* [63]. Squares denote restricted path integral Monte Carlo calculations by Pierleoni *et al.* [64].

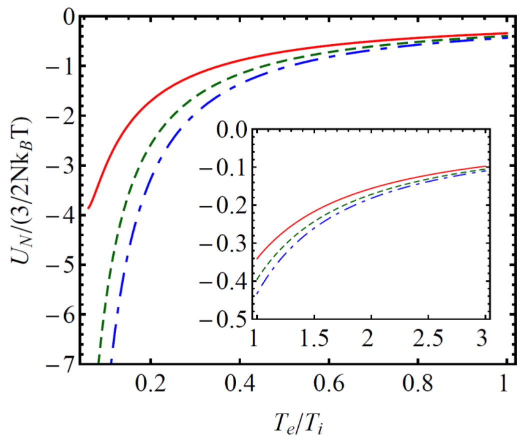

FIG. 14. (Color online) Correlation energy of nonisothermal hydrogen plasma at $r_s = 3$ and $T_e = 250\,000$ K. Solid line corresponds to the results of Sec. III A, dashed line is obtained according to (30), dashed-dotted line presents results of the Debye theory.

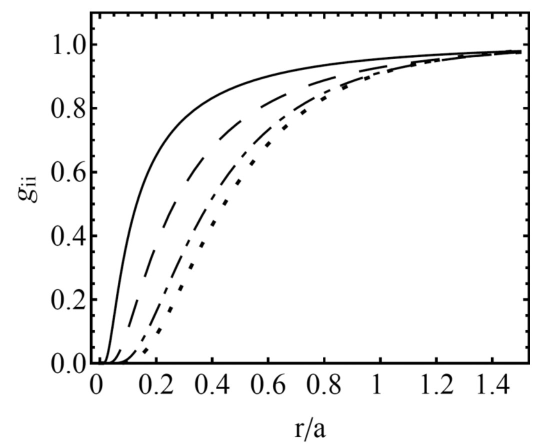

FIG. 16. Pair correlation function for ion-ion pare (12), $r_S = 1$; solid line $\Gamma = 0.1$, dashed line $\Gamma = 0.25$; Dash-dotted line $\Gamma = 0.5$; dotted line $\Gamma = 0.7$.

Pierleoni *et al.* [64] at larger values of the coupling parameter our results still have a correct behavior.

Finally, in Figs. 14 and 15 the correlation energy and the excess part of the equation of state for the nonisothermal plasma are shown. As the ratio T_e/T_i decreases, the absolute value of both the correlation energy and the excess part of the equation of state for nonisothermal plasma increase.

IV. CONCLUSION

Using the method of the dielectric response function and the potential interaction with the account of the wave nature of the electron at small distances, we obtained the effective interaction potentials for nonideal dense electron-ion plasmas. These effective potentials can be used for nonisothermal and isothermal plasmas. The expressions for the effective potential for ion interactions in plasmas with a strongly nonideal ionic subsystem and semiclassical weakly nonideal electron subsystem were obtained. Based on the effective interaction potentials, analytical expressions for the internal energy and the equation of state for a fully ionized plasma were derived. The term $\sim e^2$ in the internal energy and in the equation of state disappears when $\lambda_{ee} \to 0, \lambda_{ei} \to 0$ in agreement with the recent work of Kraeft, Kremp, and Reopke [65]. It is found that due to the symmetry effect the additional term $\sim n_e k_B T\,(n_e \lambda_{ee}^3)$ in the inner energy of plasma and in the equation of state appears [see (24) and (27)].

To take into account the partial degeneracy of electrons at high densities, the electron screening parameter k_e is calculated by the formula $k_e^2 = (4e^2 m_e)/(\pi\hbar^3)\int f_e(p)dp$, where $f_e(p)$ is the Fermi distribution, and the electron temperature is replaced by the effective temperature, which is determined by the quantum kinetic energy with the contribution of Fermi energy $T_e = E_F\theta^{5/2}\int_0^\infty y^{3/2}/(\exp(y-\beta\mu)+1)\,dy$, where μ is chemical potential of electrons, $\beta = 1/(k_B T)$ and $\theta = k_B T/E_F$ is the degeneracy parameter, E_F is Fermi energy [21].

A comparison to the asymptotic theory and computer simulations suggests that the effective potentials, obtained in this paper, can be used to adequately describe the thermodynamic properties of the two-temperature dense plasma.

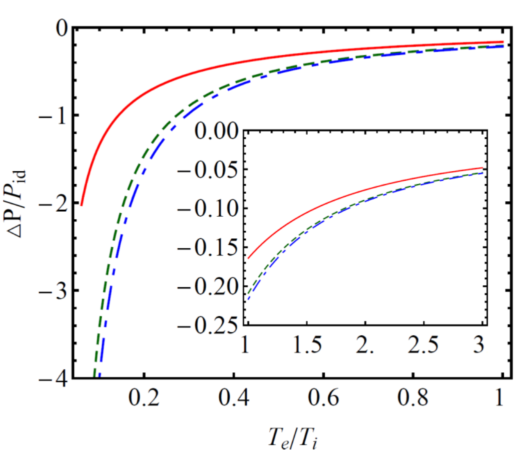

FIG. 15. (Color online) Excess part of the equation of state for nonisothermal hydrogen plasma at $r_s = 3$. Solid line corresponds to the results of Sec. III B, dashed line is obtained according to (32), dashed-dotted line presents results of the Debye correction.

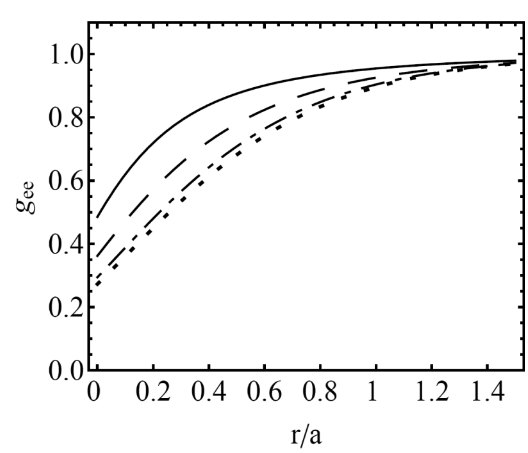

FIG. 17. Pair correlation function for electron-electron pare (13) neglecting symmetry effect, $r_S = 1$; solid line $\Gamma = 0.1$, dashed line $\Gamma = 0.25$; dash-dotted line $\Gamma = 0.5$; dotted line $\Gamma = 0.7$.

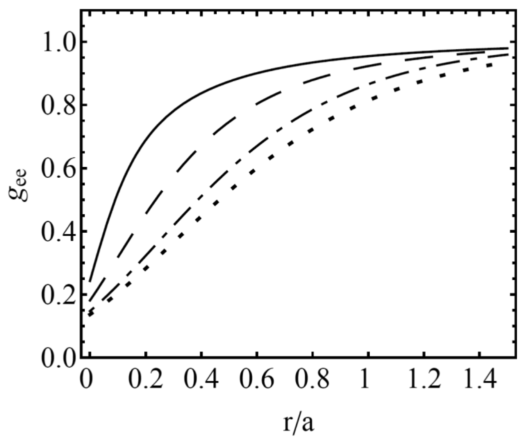

FIG. 18. Pair correlation function for an electron-electron pare (13) taking into account symmetry effect $r_S = 1$; solid line $\Gamma = 0.1$, dashed line $\Gamma = 0.25$; dashed-dotted line $\Gamma = 0.5$; dotted line $\Gamma = 0.7$.

In the case of stationary flowing plasma with a low streaming velocity the effect of dynamic screening can be taken into account by rescaling of the screening length as it was first suggested by Kremp *et al.* [66] for weakly coupled plasma. Grabowski *et al.* [67] extended their approach to strongly coupled plasmas. However, in the case of highly nonequilibrium plasma with a high streaming velocity a reliable treatment by simple rescaling of the screening length is not possible. For such systems the effective dynamic potential has strong oscillations with a deep minimum that can lead to attraction between ions [68]. A more detailed comparison of the nonrelativistic and ultrarelativistic cases is given in [69].

APPENDIX

Figures 16–21 show graphs of pair correlation function, derived from the effective interaction potential (6)

$$g_{\alpha\beta}(r) = \exp\left(-\frac{\Phi_{\alpha\beta}(r)}{k_B T_{\alpha\beta}}\right). \tag{A1}$$

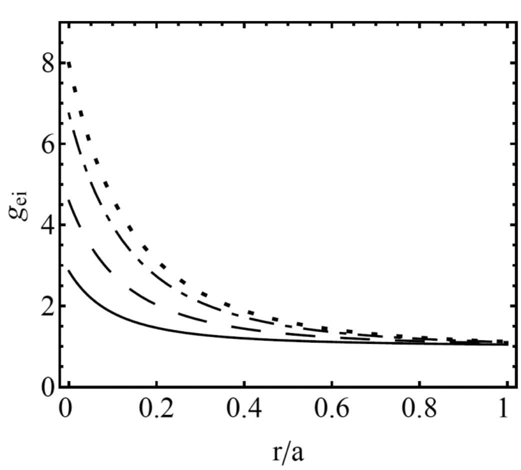

FIG. 19. Pair correlation function for an electron-ion pare (14), $r_S = 1$; solid line $\Gamma = 0.1$, dashed line $\Gamma = 0.25$; dash-dotted line $\Gamma = 0.5$; dotted line $\Gamma = 0.7$.

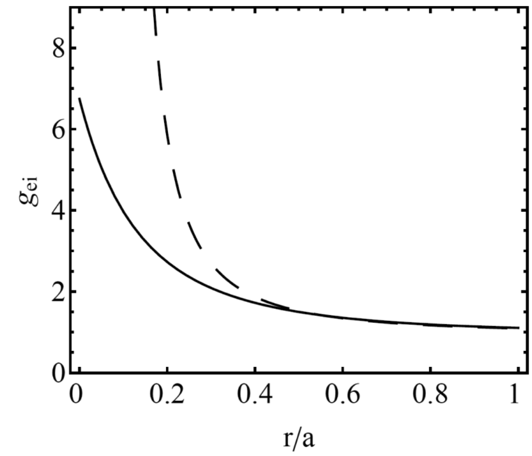

FIG. 20. Pair correlation function for an electron-ion pare (14), $\Gamma = 0.5, r_S = 1$; solid line effective potential (14), dashed line Debye potential.

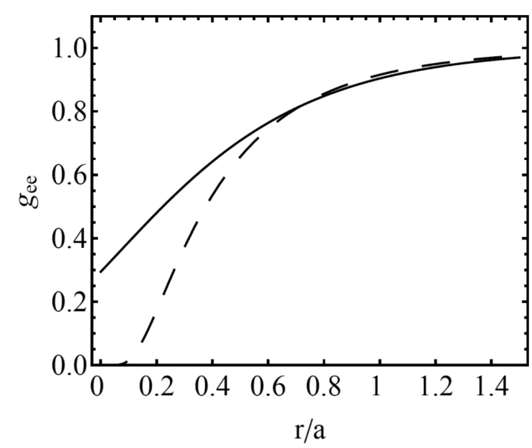

FIG. 21. Pair correlation function for an electron-electron pare (14), $\Gamma = 0.5$, $r_S = 1$; solid line effective potential (14), dashed line Debye potential.

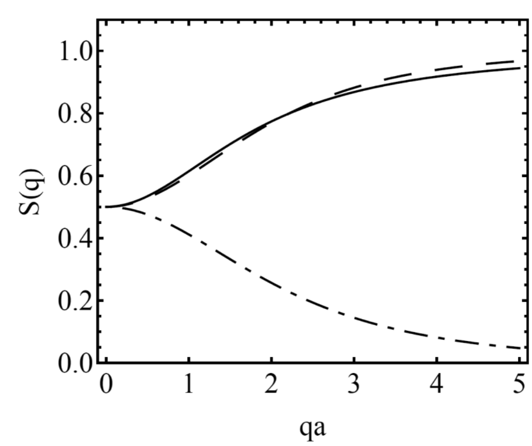

FIG. 22. Structural factor for an electron-electron pare (dashed line), an ion-ion pare (solid line), and an electron-ion pare (dash-dotted line); $T_e/T_i = 1$, $\Gamma = 0.5$, $r_S = 1$.

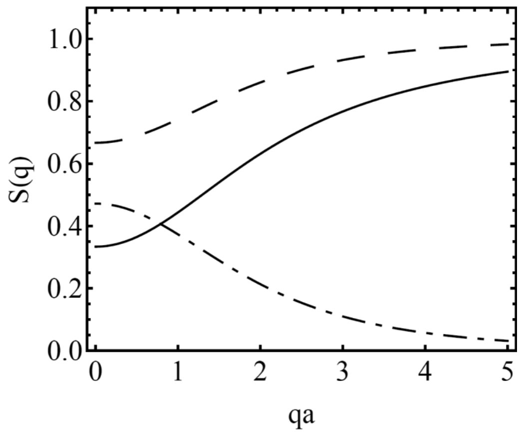

FIG. 23. Structural factor for an electron-electron pare (dashed line), an ion-ion pare (solid line), and an electron-ion pare (dashed-dotted line); $T_e/T_i = 2$, $\Gamma = 0.5$, $r_S = 1$.

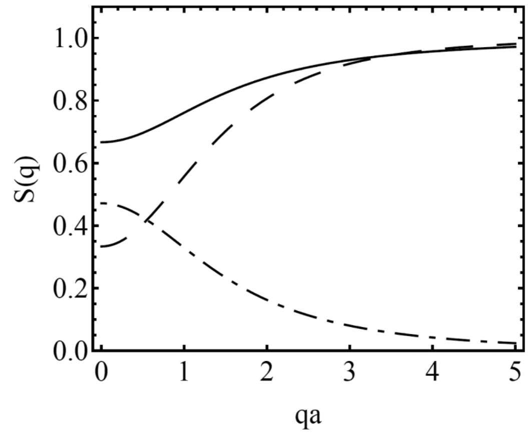

FIG. 24. Structural factor for an electron-electron pare (dashed line), an ion-ion pare (solid line), and an electron-ion pare (dash-dotted line); $T_e/T_i = 0.5$, $\Gamma = 0.5$, $r_S = 1$.

The figures show that the contribution of quantum effects gives a finite value of the pair correlation function at zero for the electron-electron and electron-ion interactions. As the coupling parameter increases, the probability of finding particles with the same charge at a given distance decreases, whereas the probability of finding particles with opposite charge increases. Accounting for the effect of symmetry in $g_{ee}(r)$ reduces the probability of finding particles at a given distance.

The Fourier transform of the effective potential enables us to calculate the structure factor directly according to the formula

$$S_{\alpha\beta}(q) = \delta_{\alpha\beta} - \frac{\sqrt{n_\alpha n_\beta}}{k_B T_{\alpha\beta}} \tilde{\Phi}_{\alpha\beta}(q). \tag{A2}$$

The Fourier transform of the effective interaction potential reads

$$\tilde{\Phi}_{\alpha\beta}(q) = \frac{4\pi e^2 Z_\alpha Z_\beta}{\lambda_{\alpha\beta}^2} \frac{\left(q^2 + 1/\lambda_{ee}^2\right)}{\left(q^2 + 1/\lambda_{\alpha\beta}^2\right)(q^2 + A^2)(q^2 + B^2)}. \tag{A3}$$

Figures 22–24 show the dependence of the structure factor for different pairs of particles for different values of T_e/T_i. To determine the electron-ion temperature, was used. The structure factor has the following long-wave asymptotics [40]:

$$S_{ee}(q \to 0) = Z\frac{T_e}{T_i} S_{ii}(q \to 0) = \sqrt{Z}\sqrt{\frac{T_e}{T_i}} S_{ei}(q \to 0). \tag{A4}$$

[1] M. French *et al.*, *Ab initio* simulations for material properties along the jupiter adiabat, Astrophys. J. Suppl. S **202**, 5 (2012).
[2] V. E. Fortov and I. N. Yakubov, *Physics of Nonideal Plasma*, (World Scientific, Singapore, 1999).
[3] T. Lower *et al.*, Uniform Multimegabar Shock Waves in Solids Driven by Laser-Generated Thermal Radiation, Phys. Rev. Lett. **72**, 3186 (1994).
[4] N. A. Tahir *et al.*, Generation of plane shocks using intense heavy ion beams: Application to Richtmyer-Meshkov instability growth studies, Phys. Plasmas **18**, 032704 (2011).
[5] E. M. Lifshitz and L. P. Pitaevskii, *Physical Kinetics* (Physmath-lit, Moscow, 2002).
[6] M. Lyon, S. D. Bergeson, and M. S. Murillo, Limit of strong ion coupling due to electron shielding, Phys. Rev. E **87**, 033101 (2013).
[7] H. Reinholz, R. Redmer, and S. Nagel, Thermodynamic and transport properties of dense hydrogen plasmas, Phys. Rev. E **52**, 5368 (1995).
[8] J. Vorberger, M. Schlanges, and W. D. Kraeft, Equation of state for weakly coupled quantum plasmas, Phys. Rev. E **69**, 046407 (2004).
[9] J. Vorberger, D. O. Gericke, and W. D. Kraeft, The equation of state for hydrogen at high densities, High Energy Density Phys. **9**, 448 (2013).
[10] C. Wang, X.-T. He, and P. Zhang, Thermophysical properties of hydrogen-helium mixtures: Re-examination of the mixing rules via quantum molecular dynamics simulations, Phys. Rev. E **88**, 033106 (2013).
[11] S. A. Khrapak, A. G. Khrapak, A. V. Ivlev, and G. E. Morfill, Simple estimation of thermodynamic properties of Yukawa systems, Phys. Rev. E **89**, 023102 (2014).
[12] A. Y. Potekhin, G. Chabrier, and F. J. Rogers, Equation of state of classical Coulomb plasma mixtures, Phys. Rev. E **79**, 016411 (2009).
[13] G. Ecker, *Theory of Fully Ionized Plasmas* (Academic Press, New York, 1972).
[14] F. B. Baimbetov, M. A. Bekenov, and T. S. Ramazanov, Effective potential of a semiclassical hydrogen plasma, Phys. Lett. A **197**, 157 (1995).
[15] F. B. Baimbetov, Kh. T. Nurekenov, and T. S. Ramazanov, Pseudopotential theory of classical non-ideal plasmas, Phys. Lett. A **202**, 211 (1995).

[16] Yu. V. Arkhipov, F. B. Baimbetov, and A. E. Davletov, Self-consistent chemical model of partially ionized plasmas, Phys. Rev. E **83**, 016405 (2011).
[17] D. Pines and Ph. Nozieres, *The Theory of Quantum Liquids* (Benjamin, New York, 1966).
[18] T. S. Ramazanov and K. N. Dzhumagulova, Effective screened potentials of strongly coupled semiclassical plasma, Phys. Plasmas **9**, 3758 (2002).
[19] T. S. Ramazanov, K. N. Dzhumagulova, and M. T. Gabdullin, Effective potentials for ion-ion and charge-atom interactions of dense semiclassical plasma, Phys. Plasmas **17**, 042703 (2010).
[20] T. S. Ramazanov, Zh. A. Moldabekov, K. N. Dzhumagulova, and M. M. Muratov, Pseudopotentials of the particles interactions in complex plasmas, Phys. Plasmas **18**, 103705 (2011).
[21] D. O. Gericke, J. Vorberger, K. Wünsch, and G. Gregori, Screening of ionic cores in partially ionized plasmas within linear response, Phys. Rev. E **81**, 065401(R) (2010).
[22] A. E. Davletov, Yu. V. Arkhipov, F. B. Baimbetov, and Zh. A. Kudyshev, Reflection index of semiclassical electron plasmas, Plasma Phys. Control. Fusion **54**, 025004 (2012).
[23] Y. V. Arkhipov, F. B. Baimbetov, A. E. Davletov, and T. S. Ramazanov, Equilibrium properties of H-Plasma, Contrib. Plasma Phys. **39**, 495 (1999).
[24] T. S. Ramazanov, K. N. Dzhumagulova, M. T. Gabdullin, A. Zh. Akbarov, and G. N. Nigmetova, Thermodynamic and transport properties of nonideal complex plasmas on the basis of Pseudopotential models, Contrib. Plasma Phys. **47**, 262 (2007).
[25] T. S. Ramazanov, M. T. Gabdullin, K. N. Dzhumagulova, and R. Redmer, Ionization equilibrium and composition of a dense partially ionized metal plasma, Contrib. Plasma Phys. **51**, 391 (2011).
[26] M. T. Gabdullin, T. S. Ramazanov, and K. N. Dzhumagulova, Composition and thermodynamic properties of dense alkali metal plasmas, Contrib. Plasma Phys. **52**, 174 (2012).
[27] M. T. Gabdullin, T. S. Ramazanov, R. Redmer, and G. B. Akhtanova, Composition of dense beryllium, boron and carbon plasmas, Contrib. Plasma Phys. **53**, 311 (2013).
[28] T. S. Ramazanov, K. N. Dzhumagulova, and A. Zh. Akbarov, Cross sections and transport coefficients of dense partially ionized semiclassical plasma, J. Phys. A: Math. Gen. **39**, 4335 (2006).
[29] T. S. Ramazanov, K. N. Dzhumagulova, and M. T. Gabdullin, Microscopic and thermodynamic properties of dense semiclassical partially ionized hydrogen plasma, J. Phys. A: Math. Gen. **39**, 4469 (2006).
[30] T. S. Ramazanov and K. M. Turekhanova, The phenomenon of runaway electrons in partially ionized non-ideal plasma, J. Phys. A: Math. Theor. **42**, 214050 (2009).
[31] T. S. Ramazanov, K. N. Dzhumagulova, M. T. Gabdullin, A. Zh. Akbar, and R. Redmer, A scattering cross-section and ionization equilibrium in dense metal plasmas, J. Phys. A: Math. Theor. **42**, 214049 (2009).
[32] C. Deutsch, Nodal expansion in a real matter plasma, Phys. Lett. A **60**, 317 (1977).
[33] C. Deutsch, Y. Furutani, and M. M. Gombert, Nodal expansions for strongly coupled classical plasmas, Phys. Rep. **69**, 85 (1981).
[34] C. Deutsch, Equilibrium properties of two-component classical plasmas, Ann. Phys. (NY) **115**, 404 (1978).
[35] A. V. Filinov, V. O. Golubnychiy, M. Bonitz, W. Ebeling, and J. W. Dufty, Temperature-dependent quantum pair potentials and their application to dense partially ionized hydrogen plasmas, Phys. Rev. E **70**, 046411 (2004).
[36] Zh. A. Moldabekov, T. S. Ramazanov, and K. N. Dzhumagulova, Pair interaction potential of particles for two-component plasma, Contrib. Plasma Phys. **52**, 207 (2012).
[37] P. Seuferling, J. Vogel, and C. Toepffer, Correlations in a two-temperature plasma, Phys. Rev. A **40**, 323 (1989).
[38] J. P. Hansen and I. R. McDonald, Microscopic simulation of a strongly coupled hydrogen plasma, Phys. Rev. A **23**, 2041 (1981).
[39] J. Hansen and I. McDonald, Thermal relaxation in a strongly coupled two-temperature plasma, Phys. Lett. A **97**, 42 (1983).
[40] R. Bredow, Th. Bornath, and W.-D. Kraeft, Hypernetted chain calculations for multi-component and nonequilibrium plasmas, Contrib. Plasma Phys. **53**, 276 (2013).
[41] G. Kelbg, Theorie des Quantenplasmas, Ann. Phys. (Leipzig) **467**, 219 (1963).
[42] K. Morawetz, Relation between classical and quantum particle systems, Phys. Rev. E **66**, 022103 (2002).
[43] M.-Y. Song and Y.-D. Jung, Quantum screening effects on the electron-ion occurrence scattering time advance in strongly coupled semiclassical plasmas, Phys. Plasmas **10**, 3051 (2003).
[44] H.-M. Kim and Y.-D. Jung, Quantum effects on polarization transport scatterings in partially ionized dense hydrogen plasmas, Phys. Plasmas **14**, 074501 (2007).
[45] D.-H. Ki and Y.-D. Jung, Quantum screening effects on the ion-ion collisions in strongly coupled semiclassical plasmas, Phys. Plasmas **17**, 074506 (2010).
[46] D.-H. Ki and Y.-D. Jung, Formation of negative hydrogen ion: Polarization electron capture and nonthermal shielding, J. Chem. Phys. **137**, 094310 (2012).
[47] D.-H. Ki and Y.-D. Jung, Influence of non-thermal shielding on the Ramsauer phenomena for the electron–atom-induced dipole scattering in Lorentzian plasmas, J. Plasma Phys. **79**, 113 (2013).
[48] P. K. Shukla and B. Eliasson, Novel Attractive Force between Ions in Quantum Plasmas, Phys. Rev. Lett. **108**, 165007 (2012).
[49] M. Bonitz, E. Pehlke, and T. Schoof, Attractive forces between ions in quantum plasmas: Failure of linearized quantum hydrodynamics, Phys. Rev. E **87**, 033105 (2013).
[50] P. K. Shukla *et al.*, Discussion on 'Novel attractive force between ions in quantum plasmas—failure of simulations based on a density functional approach', Phys. Scr. **87**, 018202 (2013).
[51] M. Bonitz, E. Pehlke, and T. Schoof, Reply to "Comment on 'Attractive forces between ions in quantum plasmas: Failure of linearized quantum hydrodynamics"', Phys. Rev. E **87**, 037102 (2013).
[52] W. Ebeling, G. E. Norman, A. A. Valuev, and I. A. Valuev, Quasiclassical theory and molecular dynamics of two-component nonideal plasmas, Contrib. Plasma Phys. **39**, 61 (1999).
[53] W. D. Kraeft, D. Kremp, W. Ebeling, and G. Röpke, *Quantum Statistics of Charged Particle Systems* (Akademie-Verlag, Berlin, 1986), p. 381.
[54] V. S. Filinov, M. Bonitz, D. Kremp, W. D. Kraeft, W. Ebeling, P. R. Levashov, and V. E. Fortov, Path integral simulations of the thermodynamic properties of quantum dense plasma, Contrib. Plasma Phys. **41**, 135 (2001).

[55] S. Tanaka and S. Ichimaru, Parametrized equation of state for dense hydrogenetic plasma, Phys. Rev. A **32**, 3756 (1985).
[56] M. Knaup, P. G. Reinhard, and C. Toepffer, Wave packet molecular dynamics simulations of deuterium in the region of laser shock-wave experiments, Contrib. Plasma Phys. **41**, 159 (2001).
[57] B. Militzer and D. M. Ceperley, Path integral Monte-Carlo calculations of the deuterium hugoniout, Phys. Rev. Lett. **85**, 1890 (2000).
[58] B. Militzer and D. M. Ceperley, Path integral Monte-Carlo simulations of the low-density hydrogen plasmas, Phys. Rev. E **63**, 066404 (2001).
[59] W. Ebeling, W. D. Kraeft, and D. Kremp, *Theory of Bound States and Ionization Equilibrium* (Akademie-Verlag, Berlin, 1976), p. 325.
[60] Yu. V. Arhipov, F. B. Baimbetov, and A. E. Davletov, Ionization equilibrium and equation of state of partially ionized hydrogen plasmas: Pseudopotential approach in chemical picture, Phys. Plasmas. **12**, 082701 (2005).
[61] H. E. DeWitt, Evaluation of the quantum mechanical ring sum with Boltzmann statistics, J. Math. Phys. **3**, 1216 (1962).
[62] J. Riemann, M. Schlages, H. E. DeWitt, and W. D. Kraeft, Equation of state of the weakly degenerate one-component plasma, Physica A **219**, 423 (1995).
[63] J. Riemann, M. Schlanges, and W. D. Kraeft, Density Expansion of the Equation of State for a Multicomponent Quantum Plasma, Laser and Particle Beams **15**, 533 (1997).
[64] C. Pierleoni, D. M. Ceperley, B. Bernu, and W. R. Magro, Equation of State of the Hydrogen Plasma by Path Integral Monte Carlo Simulation, Phys. Rev. Lett. **73**, 2145 (1994).
[65] W. D. Kraeft, D. Kremp, and G. Reopke, Direct linear term in the equation of state of plasmas, Phys. Rev. E **91**, 013108 (2015).
[66] D. Kremp, M. Schlanges, and W.-D. Kraeft, *Quantum Statistics of Nonideal Plasmas* (Springer, Berlin, 2005).
[67] P. E. Grabowski, M. P. Surh, D. F. Richards, F. R. Graziani, and M. S. Murillo, Molecular Dynamics Simulations of Classical Stopping Power, Phys. Rev. Lett. **111**, 215002 (2013).
[68] Zh. A. Moldabekov, P. Ludwig, M. Bonitz, and T. Ramazanov, Ion potential in warm dense matter: Wake effects due to streaming degenerate electrons, Phys. Rev. E **91**, 023102 (2015).
[69] Zh. A. Moldabekov, P. Ludwig, J. P. Joost, M. Bonitz, and T. Ramazanov, Dynamical screening and wake effects in classical, quantum, and ultrarelativistic plasmas, Contrib. Plasma. Phys. **55**, 186 (2015).